Journal of
Applied Remote Sensing

Simple method to determine the Priestley–Taylor parameter for evapotranspiration estimation using Albedo-VI triangular space from MODIS data

Yunjun Yao
Qiming Qin
Abduwasit Ghulam
Shaomin Liu
Shaohua Zhao
Ziwei Xu
Heng Dong

Simple method to determine the Priestley–Taylor parameter for evapotranspiration estimation using Albedo-VI triangular space from MODIS data

Yunjun Yao,[a,b] Qiming Qin,[a] Abduwasit Ghulam,[c] Shaomin Liu,[d] Shaohua Zhao,[a,e] Ziwei Xu,[d] and Heng Dong[a]

[a] Peking University, Institute of Remote Sensing and GIS, Beijing, 100871, China
[b] Beijing Normal University, College of Global Change and Earth System Science, Beijing,100875, China
[c] Saint Louis University, Department of Earth and Atmospheric Sciences and Center for Environmental Sciences, St. Louis, Missouri 63103, USA
[d] Beijing Normal University, State Key laboratory of Remote Sensing Science, School of Geography, Beijing, 100875, China
[e] Ministry of Environmental Protection, Environmental Satellite Center, Beijing, 100094, China
qmqinpku@163.com

Abstract. In this contribution, we present a simple method based on Albedo-VI (vegetation index) triangular space to determine the Priestley–Taylor parameter for estimating evaporative fraction (EF) and evapotranspiration (ET) in arid and semi-arid regions. We apply this method to MODIS and observation data acquired during the Heihe river basin field experiment from July 1 to September 30, 2008. Results show that the decreasing trend of the estimated EF from MODIS data is consistent with that of precipitation during the period of day 183 to 274, 2008. The bias of estimated daily ET deviating from the corresponding ground-measured ET is -8.66 W/m^2 and the root-mean-square error is 21.55 W/m^2, indicating the Albedo-VI triangular method has a potential in ET estimation as a simple satellite-based method independent of surface ancillary data. [DOI: 10.1117/1.3557817]

Keywords: Albedo-VI triangular space; evapotranspiration; evaporative fraction, MODIS.

Paper 10131RR received Sep. 3, 2010; revised manuscript received Jan. 14, 2011; accepted for publication Feb. 1, 2011; published online Mar. 11, 2011.

1 Introduction

Evapotranspiration (ET) is an important indicator of energy and water balance at the interface between the hydrosphere, atmosphere, and biosphere.[1,2] Accurate and temporally continuous ET estimation over large areas provides valuable means to efficient water use and sustainable management of agriculture.[3] Conventional modeling approaches or discrete point-based field observations perform reasonably well for individual sites, however, regional ET estimation accuracy is significantly hampered by spatially interpolating the limited point data due to the inherit land surface heterogeneity. Remote sensing may provide numerous land surface biophysical parameters associated with terrestrial ET, such as vegetation index (VI), albedo, land surface temperature (LST), etc. Hence the use of remote sensing data consisting of spatio-temporal samplings from space-borne sensors is a viable tool to estimate the regional latent heat flux.[4]

Much research has been done on estimating ET using remotely sensed data and meteorological observations.[5–13] These ET models mainly include the simplified empirical methods

1931-3195/2011/$25.00 © 2011 SPIE

based on the difference between surface and air temperature,[6,14] surface energy balance models (one-and two-source model, respectively),[5,15] complementary approach[16] and data assimilation in land surface models.[17] A classic and longstanding limitation associated with these methods is its dependency on some important variables such as wind speed and vapor pressure deficit that usually are not available from remote sensing data. To overcome the need for observational data, the surface temperature-vegetation index space (LST-VI) method (also referred to triangle method) has been put forward and successfully applied in certain areas for regional ET estimation.[18,19] Subsequently, Refs. 10 and 20 used thermal inertia instead of LST to estimate the evaporative fraction (EF) and ET. Similarly, Ref. 12 replaced normalized difference vegetation index (NDVI) with fractional vegetation cover from MODIS data to validate this triangular method in arid and semi-arid regions. Although great progress has been made on the remotely sensed estimation of ET on a regional scale with these triangular models, there are still challenges and limitations that have not yet been solved properly. For example, the location of a pixel in the LST-NDVI space is influenced by many factors including surface types that may have different LST/NDVI slope and intercept for equal atmospheric and surface moisture conditions.[21,22] In addition, the different LST inversion algorithms from satellite data will also affect the accuracy of LST products[23] and the final error on quantifying EF information would be magnified.

Recently, attempts have been made to explore responses of spectral feature space based on LST replaced with albedo versus VI[22] to analyze the surface drought conditions by interpreting the spatio-temporal patterns of vegetation condition albedo drought index. The hypothesis was based on the fact that there was a strong correlation between albedo and important factors of drought including LST and VI.[24,25] Generally speaking, in arid and semi-arid environments, a change in moisture availability results in a change of surface roughness and properties of the surface, which may affect the surface albedo. Considering the partition of the sensible and latent heat flux is mainly a function of moisture availability and atmospheric demand,[26] albedo is also a key parameter to determine the EF and ET. Subsequently, the Albedo-NDVI scatter plot from MODIS data had been used to construct the vegetation-albedo ratio drought index for surface drought monitoring, but had not been analyzed and validated its efficacy in ET estimation.[27]

The objectives of this paper are twofold: 1 to explore albedo-VI triangular method to determine the Priestley–Taylor parameter (a coefficient characterizing the energy partition in the Priestly–Taylor ET equation) for EF and ET estimation in arid and semi-arid regions, and 2 to validate the estimated ET from the developed algorithm with *in situ* ET measurements. The ultimate goal of this paper is developing a novel and simple algorithm to estimate regional ET.

2 Test Site and Data Collection

2.1 *Test Site Description*

The study area is located in the middle reach of the Heihe river basin, Northwestern China, with the latitude ranging from 38.11°N to 39.16°N and longitude being 99.01° to 102.06°E. Topography of the southwestern part of the study area is a mountainous region with average 3000 m above sea level and the elevation of most other areas is about 1400 m above sea level. The study area belongs to typical arid and semi-arid ecosystems. Yearly mean rainfall of this basin is approximately 174 mm and more than 73% of the annual rainfall occurs during the rainy season from June to September.[12] Figure 1 shows the International Geosphere-Biosphere Programme (IGBP) land cover types from MOD12 products that characterize the study region, and the superimposed location of the Yingke site (38.86°N, 100.41°E) chosen for this study. More details about the Yingke site and the measurements over the Heihe river basin are given at http://westdc.westgis.ac.cn/.[28]

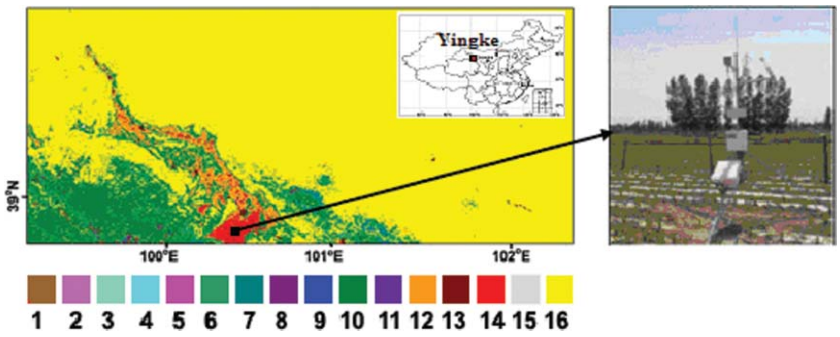

Fig. 1 Sketch map of the Yingke site in the Heihe river basin, Northwestern China. IGBP land cover types are shown: 0, water body; 1, evergreen needleleaf forest; 2, evergreen broadleaf forest; 3, deciduous needleleaf forest; 4, deciduous broadleaf forest; 5, mixed forest; 6, closed shrubland; 7, open shrubland; 8, woody savanna; 9, savanna; 10, grassland; 11, permanent wetland; 12, crop land; 13, urban/build up; 14, crop land/natural vegetation mosaic; 15, snow/ice; and 16, barren lands.

2.2 *Data Collection*

In this work, radiation flux experiments at the Yingke site located in the Heihe river basin were conducted based on the eddy covariance (ECOR) method from July 1 to September 30, 2008. The eddy covariance instruments equipped with Net radiometer, CSAT3 Campbell sonic speed device, and LI COR H_2O/CO_2 infrared analysis device are installed at a height of 2.81 m. The corresponding flux data including ET, net radiation flux (R_n), sensible heat flux (H), and near surface air temperature (T) averaged over 30 min were collected, from which daytime-averaged data used in this paper are obtained. Post-processing of the ECOR data steps include despiking, sonic temperature, and coordinate corrections. More details about the measurements and data post-processing are given in Ref. 29. Although ECOR measurements are only representative of a relatively small area (on the order of 10^2 m^2) around the ECOR site, the impacts of surface heterogeneity for such a study area is negligible in this paper. The ECOR method is considered the best for directly measuring heat fluxes in measurement experiments, but strongly advective conditions are commonplace in arid and semi-arid environments and it suffers from an energy imbalance problem.[30,31] Therefore, we selected the method proposed in Ref. 31 to correct the ET at the Yingke site.

MODIS daily reflectance products (MOD09) with a 1-km spatial resolution for 20 clear sky days (Table 1) in 2008 are chosen for little or no cloud atmosphere conditions (downloaded from https://wist.echo.nasa.gov/api).[32] MODIS reflectance products with sinusoidal projection in HDF format were then reprojected to Lat/Lon projection with GeoTIFF format using the MODIS reprojection tool (downloaded from http://lpdaac.usgs.gov/landdaac/tools/modis/index.asp).[33]

3 Methodology

3.1 *Albeod-VI Two-Dimensional Space*

A complicated relationship exists between albedo and VI (or fractional vegetation cover, F_v) for characterizing the change of surface soil moisture and heat fluxes.[21,22,34] An increase in soil moisture over the semi-arid regions will make the surface look darker with lower albedo. One may expect healthier vegetation growth for sufficient soil moisture conditions, therefore, higher VI. A reduction in the amount of the green vegetation should be associated with the increase in land surface albedo. Soil moisture content exerts the responses of albedo and VI dynamics, and their relationship changes continuously throughout the day depending upon various other factors, i.e., latent heat flux, air temperature, surface roughness, and land cover types.[4,21] Soil

Table 1 A summary of the statistics (the intercept of the dry edge, *a*, the slope of the dry edge, *b*, and the square of the correlation coefficients, R^2, of the determined dry edges for 20 clear sky days. DOY presents day of year.

DOY	*a*	*b*	R^2
183	0.42	−0.26	0.89
187	0.40	−0.20	0.91
204	0.41	−0.23	0.87
215	0.43	−0.27	0.90
216	0.39	−0.26	0.87
217	0.42	−0.24	0.89
218	0.44	−0.30	0.92
222	0.43	−0.30	0.86
223	0.42	−0.29	0.91
225	0.45	−0.33	0.88
226	0.39	−0.21	0.86
229	0.38	−0.23	0.89
234	0.40	−0.26	0.87
255	0.37	−0.25	0.90
256	0.38	−0.23	0.84
257	0.38	−0.27	0.91
258	0.39	−0.22	0.87
262	0.36	−0.24	0.87
273	0.35	−0.24	0.88
274	0.36	−0.22	0.85

moisture has a potential effect on the equilibrium between energy supply (radiation balance) and energy used (energy balance) by altering the latent heat flux in arid and semi-arid regions.[11,35] Therefore, surface radiation fluxes are also potentially affected by albedo and VI.

It has been demonstrated in the Albedo-VI scatter plots that albedo has a decreasing slope with the increase in NDVI.[22,27] Similar to LST–VI spectral space, Fig. 2 shows the diagram of the conceptual surface albedo-vegetation fraction (Albedo-F_v) triangular space. The homogeneous surfaces near the coordinate origin with sufficient water conditions (for example, water body) have the lowest albedo and VI values, and have the highest evaporation since the surfaces will evaporate more moisture. Along the ordinate (bottom-up), albedo will increase and the evaporation process fades out due to the depletion of the bare soil moisture. A wet edge (lower dashed line) represents the potential ET with sufficient water conditions and albedo decreases

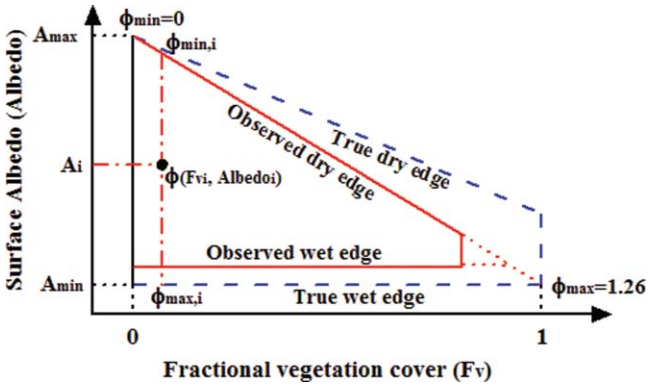

Fig. 2 Diagram of the conceptual surface albedo-vegetation fraction (Albedo-*Fv*) triangular space. The true dry edge (upper dashed line) represents the actual ET with water stressed conditions, the observed dry edge (upper solid line) representing the limiting ET, the true wet edge (lower dashed line) representing the potential ET with sufficient water conditions and the observed wet edge (lower solid line) representing the approximate potential ET.

with the increased vegetation fraction along the ordinate (left–right).[22,34,36–38] Similarly, a dry edge (upper dashed line) represents the actual ET with water stressed conditions and evaporative increases with the increasing of vegetation fraction. It should be noted that evaporation variability associated with albedo and VI is very important and, therefore, the EF is highly dependent on the albedo, VI, LST, etc. A detailed analysis of the relation of albedo and F_v with EF by deriving the Priestly–Taylor parameter (ϕ) is given in Sec. 3.2.

3.2 *Parameterization of the Priestly–Taylor parameter* ϕ

Based on the Priestly–Taylor ET equation, various LST-VI triangular methods have been used to estimate surface evaporation and soil moisture.[10,20,38] The Priestly–Taylor equation is developed from the Penman–Monteith equation[5] by assuming that the aerodynamic term can be represented by a parameter ϕ and the mathematical expression of ET is taken as follows:

$$ET = \phi(R_n - G)\frac{\Delta}{\Delta + \gamma}, \tag{1}$$

where ET is the estimated evapotranspiration (W/m^2), ϕ is a combined-effect parameter which accounts for aerodynamic resistance (dimensionless), R_n is net radiation (W/m^2), Δ is the slope of the saturated vapor pressure curve (K Pa/$^\circ$C), and γ is the psychrometric constant (K Pa/$^\circ$C).

The Priestly–Taylor parameter ϕ is a surrogate for the Priestly–Taylor constant a with wet surface equilibrium conditions.[39] a is generally interpreted as the ratio of actual evaporation to the equilibrium evaporation, and a number of studies have demonstrated this parameter may be approximated to be 1.26, even as it is empirical in nature and can vary significantly at different regions.[38,40] Generally, ϕ is derived by a two-step interpolation scheme from the dry and wet edges in the LST-VI triangular space and a detailed description can be found in Ref. 19. In this contribution, we use a slightly modified version of the two-step interpolation scheme presented in Ref. 38 to estimate ϕ in the Albedo-VI triangular space, and this interpolation scheme is consistent with the findings of Ref. 12. As depicted in Fig. 2, the value ϕ at the position $F_v = 0$ and maximum surface albedo $A_{\max}$ in the dry edge line is set to 0 ($\phi_{\min} = 0$) since the evaporation of the driest bare soil at this point is close to zero. The value of ϕcorresponding to the densest vegetation cover pixel (at the position $F_v = 1$ and the minimum surface albedo $A_{\min}$ in the dry edge line) is set to 1.26 ($\phi_{\max} = 1.26$). In our two-step interpolation scheme, the ϕvalue for any pixel $\phi(F_{vi}, \text{Albedo}_i)$ in the Albedo-F_v triangular space can easily be derived based on the following two assumptions: 1 the $\phi_{\min,i}$ value in the dry edge line for the pixel i varies linearly with F_v, namely $\phi_{\min} = 0$ at ($F_v = 0$, $A_{\max}$) and $\phi_{\max} = 1.26$ at ($F_v = 1$, $A_{\min}$). Moreover, the $\phi_{\max,i}$ value in the wet edge line for the pixel i is set to constant, namely, $\phi_{\max,i} = \phi_{\max} = 1.26$. 2. For a given F_v, the ϕvalue for a fixed pixel ϕ (F_{vi}, Albedo$_i$) decreases linearly with the increase of albedo$_i$ between $\phi_{\max,i}$ and $\phi_{\min,i}$. Thus, the $\phi_{\min,i}$ value in the dry edge line for the pixel i can be expressed as:

$$\phi_{\min,i} = 1.26F_v. \tag{2}$$

Having established the upper and lower bounds of ϕ for each F_v interval, we interpolate linearly within each F_v interval between the lowest and highest albedo. Following the illustrations in Fig. 2, the ϕ_i for a pixel at (F_{vi}, Albedo$_i$) equals:

$$\phi_i = \frac{A_{\max,i} - A_i}{A_{\max,i} - A_{\min,i}}(\phi_{\max,i} - \phi_{\min,i}) + \phi_{\min,i}, \tag{3}$$

where $\phi_{\max,i} = 1.26$, $A_{\min,i} = A_{\min}$, and $A_{\max,i} = A_{\max} - F_v(A_{\max} - A_{\min})$.

Advantages of the Albedo-VI triangular method over other complicated physical ET models are that: 1. it is easy to operate for routine, long-term mapping of ET under clear sky days,

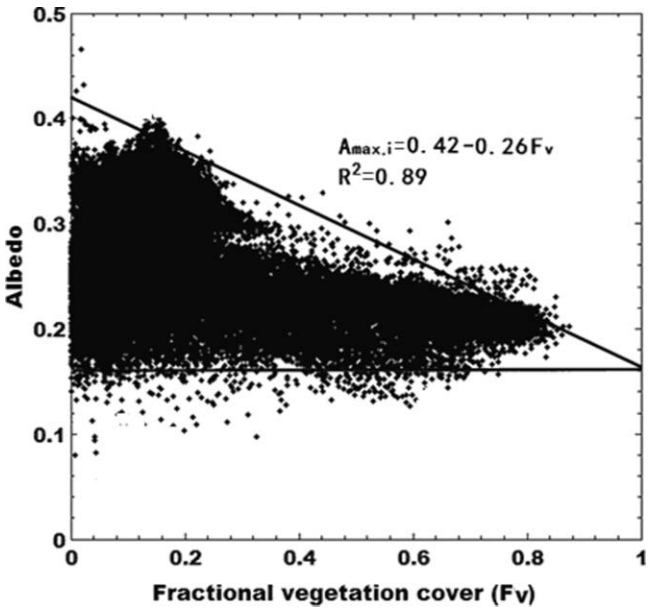

Fig. 3 An example of the dry and wet edges determination in the Albedo-F_v triangular space for MODIS data acquired on day 183, 2008.

2 albedo can be calculated from an empirical algorithm only using surface reflectance without emissivity from remotely sensed data, the Albedo-VI triangular method for Priestly–Taylor constant ϕ estimation, which uses scene-based simple empirical relations through normalization of albedo between upper (dry edge) and lower (wet edge) limits, only needs surface reflectance and air temperature data, and, 3. this avoids the computational complexities of aerodynamic resistance parameters (such as wind speed, etc). However, subjective determination of both dry and wet edges will lead to the uncertainty of $\phi$and ET estimation. In Sec. 3.3, we will illustrate the determination of both dry and wet edges in this paper.

3.3 *Determination of Dry and Wet Edges for the Albedo-VI Triangle*

VI (such as NDVI) is just a greenness variable characterizing spatial distribution of fractional vegetation cover (F_v). It presents the relative abundance of vegetation within a pixel[41], therefore, we replaced VI with F_v to construct the Albedo-VI triangular space in this paper. Previous studies, i.e., Refs. 22 and 27, have shown that the scatter plot between albedo and VI exhibits a characteristic triangular or trapezoid pattern. We constructed the Albedo and F_v scatter plots derived from MODIS data for all days of 2008 except heavily cloudy days and found triangular spaces exist for almost all clear sky days. Figure 3 shows an example of the Albedo-F_v triangular space for MODIS data for day 183, 2008 over the Heihe river basin. To estimate pixel by pixel ET using Eq. (1), both dry and wet edges in the Albedo-F_v space have to be determined first. The wet edge for such triangular space is determined by using the lowest observed clear pixel surface albedo (the albedo value for the inland water body) and all cloudy pixels fall outside of such bounds.[38] Thus the observed wet edge may be close to the true wet edge. At the same time, the lowest point of the dry edge has been determined assuming that the wet edge is the line with a constant surface albedo which is equal to that of the dry edge when $F_v = 1$. In arid and semi-arid regions, using the observed dry edge from the satellite remote sensors to represent the true dry edge for given vegetation cover may bring a bias. However, this bias should be small and is relatively unimportant in the estimation of ET. Therefore, the upper boundary of the Albedo-F_v space can be extrapolated by the warm edge seen on the diagram, which is a line

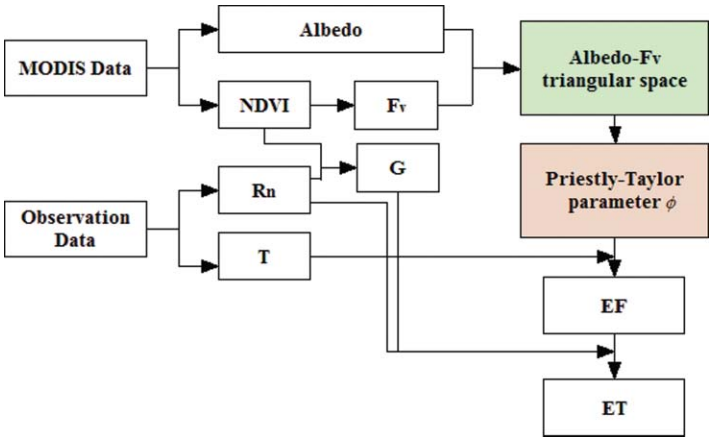

Fig. 4 Flow chart of ET estimation using the Albedo-F_v triangle method from MODIS and observation data.

through the lowest point of the dry edge using a linear regression of the observed driest points. This edge determination method can guarantee that the observed edge is closer to the theoretical true dry edge by maximizing the use of remote sensing data.

3.4 *Triangle Method Applied to MODIS and Observation Data*

Several key steps for the Albedo-F_v triangle method applied to MODIS and observation data are shown in Fig. 4, and the detailed description of each step are as follows.

3.4.1 *Calculating the fractional vegetation cover (F_v)*

NDVI is the most common index used to parameterize vegetation status from satellite data.[41] Here we replaced NDVI with F_v calculated from NDVI using the following equation:

$$F_v = \frac{\mathrm{NDVI} - \mathrm{NDVI}_{\min}}{\mathrm{NDVI}_{\max} - \mathrm{NDVI}_{\min}}, \tag{4}$$

where $\mathrm{NDVI}_{\max}$ and $\mathrm{NDVI}_{\min}$ are NDVI of full vegetation ($F_v = 1$) and bare soil ($F_v = 0$), which are set as seasonally and geographically invariant constants 0.80 and 0.15 in the study area as investigated by our research group, respectively.

3.4.2 *Surface albedo retrieval from MODIS data*

Surface albedo is the ratio of reflected to incident electromagnetic radiation, which determines how much energy is absorbed by the surface. Although the surface albedo can be obtained from the MODIS 16 day 1-km MOD43B3 product,[42] daily albedo cannot be replaced with the 16 day product due to its larger variation in different days. To reduce the complexity of albedo retrieval algorithm, we have selected the algorithm developed in Ref. 43 to retrieve the surface broadband albedo of total shortwave.

$$\mathrm{Albedo} = 0.160\rho_1 + 0.291\rho_2 + 0.243\rho_3 + 0.116\rho_4 + 0.112\rho_5 + 0.081\rho_7 - 0.0015, \tag{5}$$

where ρ_i ($i = 1,\ldots,7$) is the surface reflectance of each band from MODIS data. As an empirical equation, this algorithm may cause some biases for surface albedo retrieval and ET estimation, but our results from independent validations in Sec. 4.3 support the reliability of this algorithm with negligible biases.

3.4.3 *Net radiation flux and ground heat flux*

Surface net radiation (R_n) is the sum of incident downward and upward shortwave and longwave radiation.[44] In this paper, we directly use the upward shortwave ($S_\uparrow$), downward shortwave ($S_\downarrow$), upward longwave ($L_\uparrow$), and downward longwave ($L_\downarrow$) collected from the observed radiation flux data of the Yingke site to calculate the surface net radiation (R_n) given that R_n estimation from remotely sensed data are not the focus of our current study. R_n can be expressed as:

$$R_n = S_\downarrow - S_\uparrow + L_\downarrow - L_\uparrow. \tag{6}$$

Currently our research group is developing a new insolation radiation algorithm based on the look-up table from remotely sensed data that will make improved R_n products for regional ET estimation available in the coming years.[44,45]

Soil heat flux (G) is the energy that is conducted into (toward) the soil surface. There have been numerous reports contributing to the assessment of G using satellite derived surface biophysical variables — LST, LAI, and/or NDVI.[46] We adopt the exponential relationship between R_n and G for dense vegetation cover to acquire soil heat flux as follows.[47]

$$G = 0.058 R_n \bullet \exp(-2.03\mathrm{NDVI}). \tag{7}$$

3.4.4 *Converting the instantaneous EF to daily EF*

EF is the ratio of ET to the available energy (R_n-G) (W/m^2),[48,49] and can be directly estimated from Eq. (1).

$$EF = \phi \frac{\Delta}{\Delta + \gamma}, \tag{8}$$

since ϕ can be estimated using the Albedo-F_v triangle method from MODIS and γ is the psychrometric constant. Although γ varies as a function of ambient temperature and pressure, here we set it at a constant since its effect is usually small. Accurate Δ calculation is essential for EF estimation. Based on the near surface air temperature (T) collected from ground measurements of the Yingke site, Δ can be calculated as:

$$\Delta = \frac{26297.77}{(T + 243.5)^2} \exp\left(\frac{17.67T}{T + 243.5}\right). \tag{9}$$

EF derived from the Albedo-F_v triangle method is the instantaneous EF at noontime satellite overpass. In fact, surface ET is not limited by large scale atmospheric forcing and the partitioning of surface fluxes during daytime is mainly determined by land surface properties such as soil moisture, vegetation amount, and surface resistances.[3] Unlike surface temperature and radiant flux, they do not quite vary during the daytime, specifically, from 10 a.m. to 5 p.m. Reference[50] pointed out that soil moisture does not change significantly within a day and the difference between the instantaneous noontime EF and the EF derived from the 24-h integrated energy balance may be neglected. Reference[51] also found EF is fairly time invariant during the daytime from several *in situ* measurements. Numerous scholars verified this relative time invariant property of EF during mid-morning to late afternoon.[52] Therefore, although ET varies considerably, EF tends to be constant during the daytime hours and daily EF can be acquired from the instantaneous noontime EF. The daily EF can be expressed as:

$$\mathrm{EF}_{\mathrm{day}} = \mathrm{EF}_{\mathrm{noon}}, \tag{10}$$

where EF_{day} is the daytime evaporation fraction and EF_{noon} is the instantaneous noontime evaporation fraction.

3.5 *Comparison of ET Between Modeled Versus Simulated*

To further analyze the validity of our estimated ET in arid and semi-arid regions, we compared our estimated ET based on the Albedo-F_v triangular method with the simulated ET using a semi-empirical ET algorithm driven by net radiation, NDVI, air temperature, and diurnal air temperature range put forward by Ref. 11. The semi-empirical ET algorithm is expressed as follows:

$$\mathrm{ET} = R_n(a_0 + a_1\mathrm{NDVI} + a_2 T - a_3\mathrm{DTaR}), \tag{11}$$

where R_n is the net radiation NDVI is the normalized difference vegetation index, T is the daytime average air temperature, and DTaR is the diurnal air temperature range. a_0, a_1, and a_2 are all the empirical coefficients. This semi-empirical ET algorithm has been proved to be effective for routine, long-term estimation of ET in regional and global scale applications.

4 Results and Validation

4.1 *Albedo-F_v Scatter Plots*

The Albedo-F_v scatter plots were constructed from MODIS data to generate the ϕ by determining both dry edge and wet edge. Generally the shape of the Albedo-F_v triangular scatter plots varied widely depending on the biological and climatic settings. Previous studies[21,22,27] that documented the scatter plots represent a wide variety of surface dryness–wetness conditions. Because soil moisture has potential effects on EF, the Albedo-F_v triangle method can be successfully applied to derive ϕ and EF for ET estimation. For the Albedo-F_v triangle method, EF estimation is not only dependent on VI, but also related to albedo. The use of albedo derived from the total shortwave domain incorporated with VI would improve the accuracy of EF estimation in contrast to a single VI or albedo.

The determination of dry and wet edge in the Albedo-F_v triangle method is crucial for EF and ET estimation. Figure 5 shows the lowest surface albedo (A_{min}) at the wet edge and the highest surface albedo (A_{max}) at the dry edge retrieved from MODIS data for 20 clear sky days.

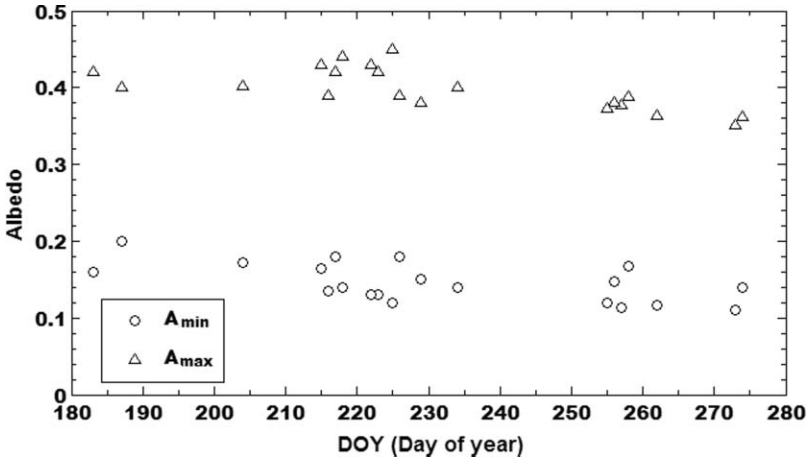

Fig. 5 The lowest surface albedo at the wet edge (A_{min}) and the highest surface albedo at the dry edge (A_{max}) from MODIS data for 20 clear-sky days.

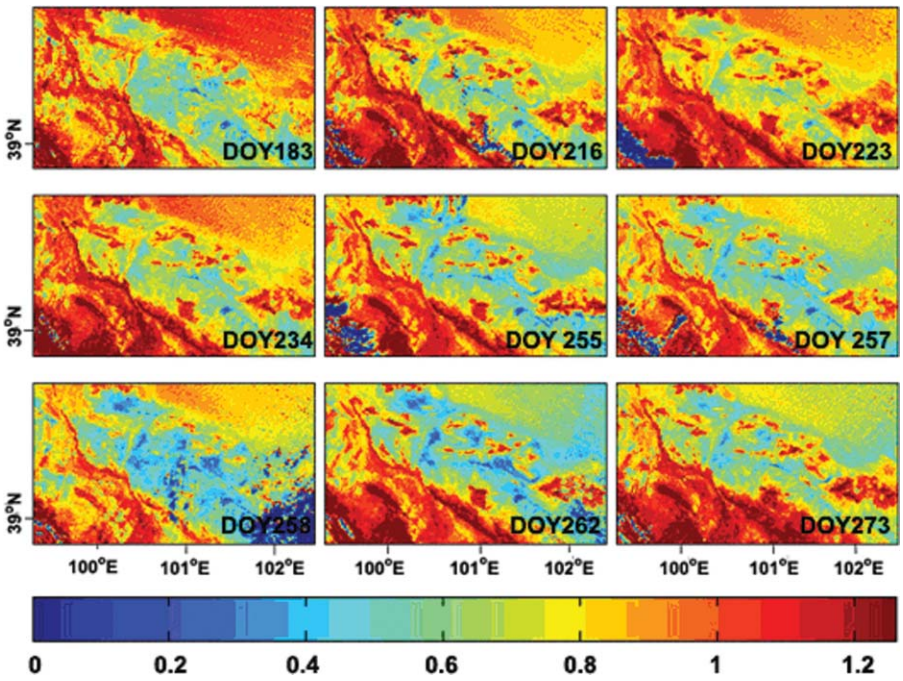

Fig. 6 Estimated Priestley–Taylor parameter (ϕ) maps using the Albedo-F_v triangular method from MODIS images of study area in 9 days (DOY 183, 216, 223, 234, 255, 257, 258, 262, and 273). DOY stands for day of year.

We can see that $A_{\min}$ varies from 0.11 (day 273) to 0.20 (day 187) and $A_{\max}$ varies from 0.35 (day 273) to 0.45 (day 225). Albedo is severely affected by the change of vegetation cover and crop senescence. The relatively high $A_{\max}$ on day 273 over the study area, therefore, may be attributed to the harvest in September. Table 1 illustrates the intercept of the dry edge (a), the slope of the dry edge (b), and the coefficient of determination (R^2) of dry edges observed for 20 clear sky days. Obviously, R^2 ranges from 0.84 to 0.92, with a mean R^2 of 0.88, indicating the reliability of our algorithm for determining the dry edge in the Albedo-F_v triangle space.

4.2 *Priestly–Taylor Parameter ϕ and Evaporative Fraction*

The Priestly–Taylor parameter ϕ can be derived based on the Albedo-F_v triangle scatter plots merely from remote sensing imagery without meteorological data. Figure 6 displays the estimated Priestley–Taylor parameter (ϕ) maps using the Albedo-F_v triangle method from MODIS images for 9 days (day 183, 216, 223, 234, 255, 257, 258, 262, and 273). One can see that along the margins between crop and barren land, ϕ varies dramatically, whereas the central region from the upper left to the lower right has constant lower values. This may be attributed to the difference between vegetation transpiration and bare soil evaporation in the study area. The average ϕ value of day 273 is obviously lower than that of day 183, indicating large variations in ϕ for different seasons due to the variations in precipitation, and this can partially explain why the ET appears to be high in the summer while it decreases in the fall.

Figure 7 illustrates the EF of the Yingke site estimated from the Priestley–Taylor parameter (ϕ) using the Albedo-F_v triangular method for 20 clear sky days. We observed that the EF varied from 0.61 (day 274) to 0.86 (day 83), with a mean EF of 0.76. The EF decreased rapidly from day 183 to day 274, which is consistent with the decreasing trend of precipitation during this period. Combining the triangle method with thermal inertia, Ref. 10 also found that the seasonal variation in the measured EF follows the rainfall pattern with a high EF for wet periods and a

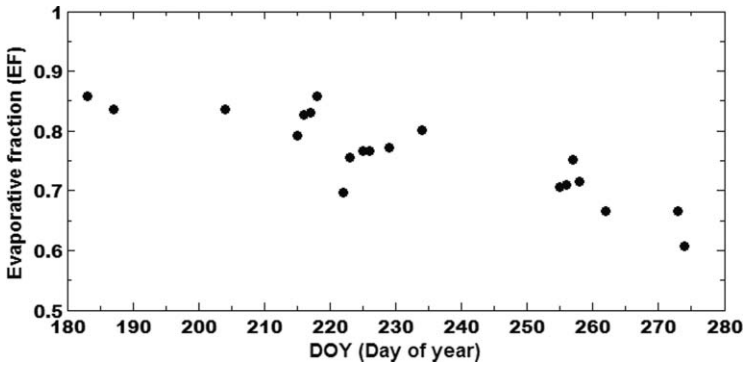

Fig. 7 EF of the Yingke site estimated from the Priestley–Taylor parameter (ϕ) using the Albedo-F_v triangular method for 20 clear sky days.

low EF for dry periods. Our results also showed that the change in precipitation may play a key role for the change of the EF, particularly in arid and semi-arid regions.

4.3 *Validation of Estimated Evapotranspiration*

Given that the accuracy of both estimated R_n and G is important for evaluating the estimated ET, we selected the ground measured R_n to reduce the error of ET estimation in this paper. Figure 8 shows the scatter plot of the estimated daily ET using the Albedo-F_v triangular method and the ground measured ET for 20 clear sky days. A bias of -8.66 W/m^2, a R^2 of 0.82 and a reasonable root mean square error (RMSE) of 21.55 W/m^2 are obtained compared to measured values. We also simulated the ET using the semi-empirical ET algorithm driven by net radiation, NDVI, air temperature, and diurnal air temperature range. Correlation analysis between the ground-measurement versus the simulated ET indicated a bias of -26.21 W/m^2, RMSE of 34.40 W/m^2, and R^2 was 0.82. Obviously the accuracy of the estimated ET using the Albedo-F_v triangular method is higher than that of the simulated ET using the semi-empirical ET algorithm. Reference[38] documented an RMSE of 85.30 W/m^2 by using the linear NDVI-LST spatial variation method from NOAA-AVHRR data, and an interpolated surface net radiation map over the Southern Great Plains in 2001. Reference[52] suggested the required ET retrieval accuracy varies among the applications over different ecosystems, but is typically around 50 W/m^2. The error magnitude from our results was well below those cited findings.

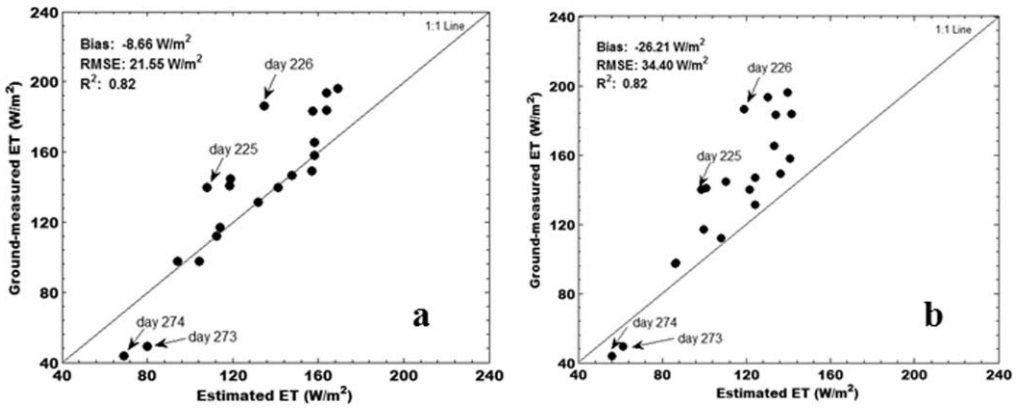

Fig. 8 Scatter plot of the estimated daily ET using (a) the Albedo-F_v triangular method, (b) the semi-empirical ET algorithm driven by net radiation, NDVI, air temperature, and diurnal air temperature range, and the ground measured ET for 20 clear sky days.

Although there is good agreement between the estimated ET using the Albedo-F_v triangular method and the ground measured ET, the large discrepancies are evident on days 225 (ΔET $= -32.12$ W/m^2), 226 (ΔET $= -51.72$ W/m^2), 273 (ΔET $= 30.58$ W/m^2), and 174 (ΔET $= 25.11$ W/m^2). Possible causes of these large biases observed on days 225 and 226 are difficult to quantify accurately due to the lack of sufficient field measurements. On days 273 and 274, the errors of albedo retrieval under the low vegetation cover conditions may lead to the inaccurate determination of dry and wet edges, causing the positive biases of estimated ET.

5 Conclusion

A new Albedo-VI triangular method was developed using broadband albedo of the total shortwave and Fv from MODIS data to determine the Priestley–Taylor parameter for ET estimation in arid and semi-arid regions. This method can be used to estimate the EF using remotely sensed data, and no additional ancillary field measurements are required, therefore, it avoids the computational complexities of aerodynamic resistance parameters. The results showed that the decreasing trend of the estimated EF from MODIS data was consistent with that of precipitation during the period of day 183 to 274, 2008. The result of daily estimated and ground-measured ET using ground observation data collected from the Yingke site shows that there is good agreement between them, indicating the Albedo-VI triangular method may provide a reliable estimation of ET in arid and semi-arid regions.

It should be noted that accurate determination of dry and/or wet edges is important in the estimation of ϕ and ET, and therefore, can be a challenging aspect. Although the wet edge can be determined by using the lowest observed surface albedo corresponding to clear pixels, the true wet edge cannot be easily acquired in arid and semi-arid areas due to the fact that finding potentially evaporating pixels in these climate regions is difficult.[12] Additional studies and validations are needed to reach a solid conclusion.

Acknowledgments

The authors thank the anonymous reviewers for their critical and helpful comments and suggestions. The authors would also like to thank Professor Shunlin Liang and Dr. Kaicun Wang from University of Maryland, for their help. This work was partially supported by the Natural Science Fund of China (No. 40771148), the R&D Special Fund for Public Welfare Industry of China (Meteorology) (No. GYHY200806022), the High-Tech Research and Development Program of China (Nos. 2008AA121806–04 and 2009AA12Z128).

References

1. C. H. B. Priestley and R. J. Taylor, "On the assessment of surface heat flux and evaporation using large-scale parameters," *Mon. Weather Rev.* **100**(2), 81–92 (1972).
2. R. R. Nemani, M. A. White, P. Thornton, K. Nishida, S. Reddy, J. Jenkins, and S. W. Running, "Recent trends in hydrologic balance have enhanced the carbon sink in the United States," *Geophys. Res. Lett.* **29**(10), 1468–1471 (2002).
3. L. Jiang, S. Islam, W. Guo, A. S. Jutla, S. U. S Senarath, B. H. Ramsay, and E. Eltahir, "A satellite-based daily actual evapotranspiration estimation algorithm over South Florida," *Glob. Planet. Change* **67**(1–2), 62–77 (2009).
4. K. Mallick, B. K. Bhattacharya, V. U. M. Rao, D. R. Reddy, S. Banerjee, H. Venkatesh, V. Pandey, G. Kar, J. Mukherjee, S. P. Vyas, A. S. Gadgil, and N. K. Patel, "Latent heat flux estimation in clear sky days over Indian agroecosystems using noontime satellite remote sensing data," *Agric. Forest Meteorol.* **149**(10), 1646–1665 (2009).
5. J. L. Monteith, "Evaporation and the environment," in *Fogg GE (ed) The State and Movement of Water in Living Organisms, 19th Symposium of the Society for Experimental Biology*, University Press, Cambridge, pp. 205–234 (1965).

6. B. Seguin and B. Itier, "Using midday surface temperatures to estimate daily evaporation from satellite thermal IR data," *Int. J. Remote Sens.* **4**, 371–383 (1983).
7. M. C. Anderson, J. M. Norman, G. R. Diak, W. P. Kustas, and J. R. Mecikalski, "A two-source time-integrated model for estimating surface fluxes from thermal infrared satellite observations," *Remote Sens. Environ.* **60**, 195–216 (1997).
8. J. M. Norman, M. C. Anderson, W. P. Kustas, A. N. French, J. R. Mecikalski, R. D. Torn, G. R. Diak, T. J. Schmugge, and B. C. W. Tanner, "Remote sensing of surface energy fluxes at 10^1-m pixel resolutions," *Water Resour. Res.* **39**(8), 1221–1237 (2003).
9. Q. Z. Mu, F. A. Heinsch, M. S. Zhao, and S. W. Running, "Development of a global evapotranspiration algorithm based on MODIS and global meteorology data," *Remote Sens. Environ.* **111**(4), 519–536 (2007).
10. S. Stisen, I. Sandholt, A. Nørgaard, R. Fensholt, and K. H. Jensen, "Combining the triangle method with thermal inertia to estimate regional evapotranspiration-Applied to MSG-SEVIRI data in the Senegal River basin," *Remote Sens. Environ.* **112**(3), 1242–1255 (2008).
11. K. C. Wang and S. L. Liang, "An improved method for estimating global evapotranspiration based on satellite determination of surface net radiation, vegetation index, temperature, and soil moisture," *J. Hydrometeo.* **9**(4), 712–727 (2008).
12. R. L. Tang, Z. L. Li, and B. H. Tang, "An application of the T_s-VI triangle method with enhanced edges determination for evapotranspiration estimation from MODIS data in arid and semi-arid regions: Implementation and validation," *Remote Sens. Environ.* **114**, 540–551 (2010).
13. Y. J. Yao, S. L. Liang, Q. M. Qin, K. C. Wang, and S. H. Zhao, "Monitoring global land surface drought based on a hybrid evapotranspiration model," *Int. J. Appl. Earth Obs. Geoinf.*, in press (2010).
14. K. C. Wang, P. C. Wang, Z. Q. Li, M. Cribb, and M. Sparrow, "A simple method to estimate actual evapotranspiration from a combination of net radiation, vegetation index, and temperature," *J. Geophys. Res.* **112**(D15), D15107 (2007).
15. W. J. Shuttleworth and J. S. Wallace, "Evaporation from sparse crops-an energy combination theory," *Q. J. R. Meteorol. Soc.* **111**, 839–855 (1985).
16. R. J. Granger, "A complementary relationship approach for evaporation from non-saturated surfaces," *J. Hydrol.* **111**, 31–38 (1989).
17. G. Boni, D. Entekhabi, and F. Castelli, "Land data assimilation with satellite measurements for the estimation of surface energy balance components and surface control on evaporation," *Water Resour. Res.* **37**, 1713–1722 (2001).
18. J. C. Price, "Using spatial context in satellite data to infer regional scale evapotranspiration," *IEEE Trans. Geosci. Remote Sens.* **28**, 940–948 (1990).
19. L. Jiang and S. Islam, "A methodology for estimation of surface evapotranspiration over large areas using remote sensing observations," *Geophys. Res. Lett.* **26**, 2773–2776 (1999).
20. K. C. Wang, Z. Q. Li, and M. Cribb, "Estimation of evaporative fraction from a combination of day and night land surface temperature and NDVI: A new method to determine the Priestley-Taylor parameter," *Remote Sens. Environ.* **102**(3–4), 293–305 (2006).
21. I. Sandholt, K. Rasmussen, and J. Andersen, "A simple interpretation of the surface temperature-vegetation index space for assessment of surface moisture status," *Remote Sens. Environ.* **79**(2–3), 213–224 (2002).
22. A. Ghulam, Z. Li, Q. Qin, and Q. Tong, "Exploration of the spectral space based on vegetation index and albedo for surface drought estimation," *J. Appl. Remote Sens.* **1**, 013529 (2007).
23. S. H. Zhao, Q. M. Qin, Y. H. Yang, Y. J. Xiong, and G. Y. Qiu, "Comparison of two split-window methods for retrieving land surface temperature from MODIS data," *J. Earth Syst. Sci.* **118**(4), 345–353 (2009).
24. D. O. Fuller and C. Ottke, "Land cover, rainfall and land-surface albedo in West Africa," *Clim. Change.* **54**(1–2), 181–204 (2002).

25. A. Ghulam, Q. Qiming, Z. Zhan, and Z. Li, "Albedo variation and its effects on surface biophysical and climate factors," in *The 9th International Symposium on Physical Measurements and Signatures in Remote Sensing (ISPMSRS)*, Beijing, China, Oct. 17–19, 2005.
26. J. G. Alfieri, P. D. Blanken, D. N. Yates, and K. Steffen, "Variability in the environmental factors driving evapotranspiration from a grazed rangeland during severe drought conditions," *J. Hydrometeorol.* **8**, 207–220 (2007).
27. Y. J. Yao, Q. M. Qin, L. Zhu, and N. Yang, "Relating albedo and vegetation index with surface dryness using Landsat ETM+ imagery," in *The IEEE International Geoscience and Remote Sensing Symposium (IGARSS)*, Boston, MA, July 7–11, 2008.
28. http://westdc.westgis.ac.cn/.
29. Z. W. Xu, S. M. Liu, L. J. Gong, J. M. Wang, and X. W. Li, "A study on the data processing and quality assessment of the Eddy Covariance System," *Adv. Earth Planet Sci.* **23**(4), 357–370 (2007) [In Chinese].
30. D. Baldocchi, E. Falge, L. H. Gu, R. Olson, D. Hollinger, S. Running, P. Anthoni, C. Bernhofer, K. Davis, R. Evans, J. Fuentes, A. Goldstein, G. Katul, B. Law, X. H. Lee, Y. Malhi, T. Meyers, W. Munger, W. Oechel, K. T. Paw, U. K. Pilegaard, H. P. Schmid, R. Valentini, S. Verma, T. Vesala, K. Wilson and S. Wofsy, "FLUXNET: A new tool to study the temporal and spatial variability of ecosystem-scale carbon dioxide, water vapor and energy flux densities," *Bull. Am. Meteorol. Soc.* **82**(11), 2415–2434 (2001).
31. T. E. Twine, W. P. Kustas, J. M. Norman, D. R. Cook, P. R. Houser, T. P. Meyers, J. J. Prueger, P. J. Starks, and M. L. Wesely, "Correcting eddy-covariance flux underestimates over a grassland," *Agric. Forest Meteorol.* **103**(3), 279–300 (2000).
32. https://wist.echo.nasa.gov/api/.
33. http://lpdaac.usgs.gov/landdaac/tools/modis/index.asp.
34. R. T. Gillies, T. N. Carlson, J. Cui, W. P. Kustas, and K. S. Humes, "A verification of the 'triangle' method for obtaining surface soil water content and energy fluxes from remote measurements of the Normalized Difference Vegetation Index (NDVI) and surface radiant temperatures," *Int. J. Remote Sens.* **18**(15), 3145–3166 (1997).
35. M. Detto, N. Montaldo, J. D. Albertson, M. Mancini, and G. Katul, "Soil moisture and vegetation controls on evapotranspiration in a heterogeneous Mediterranean ecosystem on Sardinia, Italy," *Water Resour. Res.* **42**(8), W08419 (2006).
36. T. N. Carlson, R. R. Gillies, and E. M. Perry, "A method to make use of thermal infrared temperature and NDVI measurements to infer surface soil water content and fractional vegetation cover," *Int. J. Remote Sens.* **9**, 161–173 (1994).
37. E. G. Lambin and D. Ehrlich, "The surface temperature-vegetation index space for land cover and land-cover change analysis," *Int. J. Remote Sens.* **17**(3), 463–487 (1996).
38. L. Jiang and S. Islam, "Estimation of surface evaporation map over Southern Great Plains using remote sensing data," *Water Resour. Res.* **37**(2), 329–340 (2001).
39. W. E. Eichinger, M. B. Parlange, and H. Stricker, "On the concept of equilibrium evaporation and the value of the Priestley-Taylor coefficient," *Water Resour. Res.* **32**, 161–164 (1996).
40. W. P. Kustas, D. I. Stannard, and K. J. Allwine, "Variability in surface energy flux partitioning during Washita'92: Resulting effects on Penman-Monteith and Priestly-Taylor parameters," *Agric. Forest Meteorol.* **82**, 171–193 (1996).
41. C. J. Tucker, "Red and photographic infrared linear combination for monitoring vegetation," *Remote Sens. Environ.* **8**, 127–150 (1979).
42. C. B. Schaaf, F. Gao, A. H. Strahler, W. Lucht, X. W. Li, T. Tsang, N. C. Strugnell, X. Y. Zhang, Y. F. Jin, J. P. Muller, P. Lewis, M. Barnsley, P. Hobson, M. Disney, G. Roberts, M. Dunderdale, C. Doll, R. P. d'Entremont, B. X. Hu, S. L. Liang, J. L. Privette, and D. Roy, "First operational BRDF, albedo nadir reflectance products from MODIS," *Remote Sens. Environ.* **83**(1–2), 135–148 (2002).
43. S. Liang, "Narrowband to broadband conversions of land surface albedo 1 Algorithm," *Remote Sens. Environ.* **76**(2), 213–238 (2000).

44. K. C. Wang and S. L. Liang, "Estimation of surface net radiation from solar shortwave radiation measurements," *J. Appl. Meteor. Climatol.* **48**(3), 634–643 (2009).
45. S. Liang, T. Zheng, R. Liu, H. Fang, S. C. Tsay, and S. Running, "Estimation of incident photosynthetically active radiation from Moderate Resolution Imaging Spectrometer data," *J. Geophys. Res.* **111**(D15), D15208 (2006).
46. R. G. Allen, M. Tasumi, and R. Trezza, "Satellite-based energy balance for mapping evapotranspiration with internalized calibration (METRIC)-model," *J. Irrig. Drain. Eng.* **133**, 380–394 (2007).
47. R. J. Reginato, R. F. Jackson, and P. J. Pinter, "Evapotranspiration calculated from remote multispectral and ground station meteorological data," *Remote Sens. Environ.* **18**, 75–89 (1985).
48. W. J. Shuttleworth, R. J. Gurney, A. Y. Hsu, and J. P. Ormsby, "FIFE: The variation in energy partition at surface flux sites; remote sensing and large-scale global processes (Proceedings of the IAHS Third Int. Assembly, Baltimore, MD, May 1989)," *IAHS Publ.* **186**, 67–74 (1989).
49. K. Nishida, R. R. Nemani, S. W. Running, and J. M. Glassy, "An operational remote sensing algorithm of land surface evaporation," *J. Geophys. Res.* **108**(D9), 4270–4283 (2003).
50. R. D. Crago and W. Brutsaert, "Conservation and variability of the evaporative fraction during the daytime," *J. Hydrol.* **180**(1–4), 173–194 (1996).
51. W. Brutsaert and D. Chen, "Diurnal variation of surface fluxes during thorough drying (or severe drought) of natural prairie," *Water Resour. Res.* **32**, 2013–2019 (1996).
52. B. Seguin, F. Becker, T. Phulpin, X. F. Gu, G. Guyot, Y. Kerr, C. King, J. P. Lagouarde, C. Ottlé, M. P. Stoll, A. Tabbagh and A. Vidal, "IRSUTE: A mini-satellite project for land surface heat flux estimation from field to regional scale," *Remote Sens. Environ.* **68**, 357–369 (1999).

YunjunYao is a PhD candidate at Peking University in China. He received his MS degree in physical geography from Beijing Normal University, China in 2005. He is currently pursuing his research as a junior research scientist at College of Global Change and Earth System Science, Beijing Normal University, China. His research interests include estimation of evapotranspiration and retrieval of surface biophysical parameters by remote sensing.

Qiming Qin is a professor at Peking University in China. He received his PhD. degree in cartography and GIS from Peking University, China in 1990. He is the author of more than 90 journal papers and has written 4 book chapters. His current research interests focus on retrieval of surface biophysical parameters by remote sensing.

Abduwasit Ghulam is an assistant research professor at Saint Louis University. He received his PhD degree in cartography and GIS from Peking University, China in 2006. He has authored more than 30 journal papers, and presented numerous national/international conferences and workshops, and written a book chapter. His current research interests include retrieval of surface biophysical parameters by remote sensing, InSAR/DInSAR, and monitoring tropical forest health using polarimetric SAR.

Shaomin Liu is a professor at the School of Geography, Beijing Normal University, China. He received his PhD degree in meteorology from China Agricultural University, China in 2001. His current research interests focus on surface flux observations and assimilation from different sources and numerical models.

Shaohua Zhao is a postdoctoral research associate at Peking University in China. He received his PhD degree in physical geography from Beijing Normal University, China in 2008. His research interests include estimation of evapotranspiration, retrieval of soil moisture based on remote sensing and GIS, and natural hazards monitoring.

Ziwei Xu is an assistant research scientist at the School of Geography, Beijing Normal University, China. He received his PhD degree in cartography and GIS from Beijing Normal University, China in 2009. His current research interests include surface flux observations and data analysis.

Heng Dong is a PhD candidate at Peking University in China. He received his BS degree in surveying and mapping from Wuhan University of Technology, China in 2008. His current research interests include farmland drought monitoring and retrieval of surface biophysical parameters by remote sensing.